Matrix Pseudospectral Method for Elastic Tides Modeling of Planetary Bodies

Eliška Zábranová, Ladislav Hanyk and Ctirad Matyska

Department of Geophysics
Faculty of Mathematics and Physics
Charles University
V Holešovičkách 2, 180 00 Prague 8, Czech Republic

Abstract

Deformations and changes of the gravitational potential of prestressed elastic bodies caused by the tidal forces are described by means of the momentum equation, the Poisson equation and the constitutive relation. For the case of spherical symmetry we review how the equations and boundary conditions are decomposed into a series of boundary value problems (BVP) for ordinary differential equations of the second order. In contrast to traditional Runge-Kutta integration techniques, highly accurate pseudospectral schemes are employed to directly discretize the BVP on Chebyshev grids and a set of linear algebraic equations with an almost block diagonal matrix is derived. Both the accuracy and efficiency of the method are tested by evaluating the tidal Love numbers for the Earth's model PREM. Finally, the tidal Love numbers for models of Mars and Venus are calculated and perspectives of the method are outlined.

1. Introduction

Computations of the response of a (visco)elastic selfgravitating body to external or internal forces (tides, postglacial rebound, free oscillations) have a long history that goes back to the 19^{th} century with first attempts to describe the oscillations of an elastic sphere by S. D. Poisson, H. Lamb and A. E. H. Love. Nowadays the general Lagrangian theory exists, provides the mathematical description of these phenomena by means of appropriate partial differential equations together with sufficiently accurate boundary conditions and seems to be quite satisfactory (e.g., Dahlen and Tromp 1998). However, new numerical methods enabling us to solve these equations in an effective way are still being developed (Martinec 1999; Martinec 2000; Kobayashi 2007) and this paper represents a continuation of our previous effort in this research (Hanyk 1999; Hanyk et al. 2002; Zábranová 2008).

Here we will confine ourselves to the elastic response of planetary bodies to tidal forcing and start our considerations with the traditional description of deformations and perturbations of gravitational potential in a prestressed selfgravitating elastic body (e.g., Martinec 1984; Dahlen and Tromp 1998), where general equations of motion coupled with the Poisson equation for incremental field variables can be found. In the case of a spherically symmetric model, spherical harmonic decomposition of field variables is used and the spheroidal deformations together with gravitational-potential perturbations are then described by a series of systems of three ordinary differential equations (ODEs) of the 2^{nd} order. Traditional numerical solution of these ODEs is based on its transformation to the system of six ODEs of the 1^{st} order (Melchior 1978) having three linearly independent bounded (in the center of the models) solutions. The Runge-Kutta integration technique is employed to find these solutions numerically, which are then linearly combined to adjust corresponding boundary conditions at the Earth's surface.

The classical approach based on the Runge-Kutta integration is rather cumbersome, especially for the free elastic oscillation calculations, when the corresponding eigenproblem is solved. This is the reason why we have returned to the original system of three 2^{nd}-order ODEs and propose to solve the corresponding BVP directly by means of a finite-difference scheme with a pseudospectral accuracy designed by Fornberg (1996). Here we will demonstrate the applicability of such an approach to the calculations of the tidal Love numbers for the Earth, Mars and Venus.

2. Governing set of partial differential equations

In this section we formulate the partial differential equations (PDEs) and the boundary conditions, which describe the response of a prestressed selfgravitating elastic model to an external gravitational force, i.e., temporal behavior of the displacement and the incremental gravitational potential in the entire body. The referenced unperturbed state of our model—the hydrostatic equilibrium—is described by the momentum equation,

$$\nabla \cdot \boldsymbol{\tau_0} + \boldsymbol{f_0} = \boldsymbol{0}, \tag{1}$$

where $\boldsymbol{\tau_0}$ represents the Cauchy stress tensor and the forcing term satisfies $\boldsymbol{f_0} = -\rho_0 \nabla \varphi_0$, ρ_0 is the reference density. The hydrostatic gravitational potential φ_0 fulfills the Poisson equation,

$$\Delta \varphi_0 = 4\pi G \rho_0, \tag{2}$$

where G is the Newton gravitational constant. The boundary conditions in the reference state, required at the surface and all internal boundaries, are the continuity of the normal traction, the gravitational potential and the normal component of its gradient; moreover, the tangential traction vanishes at the surface and at liquid boundaries.

The complete system of PDEs for the displacement $\boldsymbol{u}$, the incremental gravitational potential φ and the incremental stress tensor $\boldsymbol{\tau}$ consists of the momentum equation, the Poisson equation and the constitutive relation,

$$\nabla \cdot \boldsymbol{\tau} - \rho_0 \nabla \varphi + \nabla \cdot (\rho_0 \boldsymbol{u}) \nabla \varphi_0 - \nabla (\rho_0 \nabla \varphi_0 \cdot \boldsymbol{u}) = \rho_0 \frac{\partial^2 \boldsymbol{u}}{\partial t^2}, \tag{3}$$

$$\nabla \cdot (\nabla \varphi + 4\pi G \rho_0 \boldsymbol{u}) = 0, \tag{4}$$

$$\lambda \nabla \cdot \boldsymbol{u} \boldsymbol{I} + \mu \left[\nabla \boldsymbol{u} + (\nabla \boldsymbol{u})^{\mathrm{T}} \right] = \boldsymbol{\tau}, \tag{5}$$

where λ and μ are the elastic Lamé parameters, the latter also referred to as the shear modulus. This Lagrangian-Eulerian system of equations can be found in, e.g., Martinec (1984) or Dahlen and Tromp (1998).

Lagrangian boundary conditions have to be added to the PDEs (3)–(5) on the surface of the model and on the internal boundaries. On the solid-solid boundary the displacement and the incremental traction are continuous,

$$[\boldsymbol{u}]_-^+ = \boldsymbol{0}, \tag{6}$$

$$[\boldsymbol{\tau} \cdot \boldsymbol{n}]_-^+ = \boldsymbol{0}, \tag{7}$$

where $\boldsymbol{n}$ is the unit vector normal to the boundaries. On the liquid boundary the normal component of the both displacement and the incremental traction are continuous and the tangential components of the traction vanish,

$$[\boldsymbol{u} \cdot \boldsymbol{n}]_-^+ = 0, \tag{8}$$

$$[\boldsymbol{\tau} \cdot \boldsymbol{n} \cdot \boldsymbol{n}]_-^+ = 0, \tag{9}$$

$$\boldsymbol{\tau} - (\boldsymbol{\tau} \cdot \boldsymbol{n})\, \boldsymbol{n} = \boldsymbol{0}. \tag{10}$$

Let us emphasize that the relation (10) represents four independent equations since it holds on each side of the boundary. On the free surface both the normal and tangential components of the incremental traction vanish,

$$\boldsymbol{\tau} \cdot \boldsymbol{n} = \boldsymbol{0}. \tag{11}$$

The displacement vector and the incremental gravitational potential are zero at the center of the model,

$$\boldsymbol{u} = \boldsymbol{0}, \tag{12}$$

$$\varphi = 0. \tag{13}$$

On all boundaries the Eulerian incremental potential is continuous, whereas there are jumps of the normal component of its gradient because the boundary undulations are replaced by apparent surface mass densities,

$$[\varphi]_-^+ = 0, \tag{14}$$

$$[\nabla \varphi \cdot \boldsymbol{n} + 4\pi G \rho_0 \boldsymbol{u} \cdot \boldsymbol{n}]_-^+ = 0. \tag{15}$$

This is the way how the geometry of the body remains unchanged during deformations also in the description of the gravitational potential, which is treated by means of an Eulerian formalism. The geometry of the domain, where the momentum equation (3) is solved, is fixed implicitly since a Lagrangian formalism is employed for deformations.

3. Spherical harmonic decomposition

We consider spherically symmetric models in what follows. In order to employ the spherical symmetry, we use a formalism of spherical harmonic functions for individual quantities. Let $(\boldsymbol{e}_r, \boldsymbol{e}_\vartheta, \boldsymbol{e}_\phi)$ be the unit spherical vector basis with the radius r, the colatitude $\vartheta \in \langle 0, \pi \rangle$ and the longitude $\phi \in \langle 0, 2\pi \rangle$. On the unit sphere a quadratically integrable function can be decomposed by means of the complete orthonormal basis of spherical harmonic functions $Y_{nm}(\vartheta, \phi)$,

$$f(r, \vartheta, \phi) = \sum_{n=0}^{\infty} \sum_{m=-n}^{n} f_{nm}(r) Y_{nm}(\vartheta, \phi), \tag{16}$$

where n is the degree, m the order and $f_{nm}(r)$ are coefficients of the expansion. The spherical harmonic functions are defined by the relation

$$Y_{nm}(\vartheta, \phi) = (-1)^m N_{nm} P_n^m(\cos\vartheta) \mathrm{e}^{(im\phi)}, \tag{17}$$

where N_{nm} are the norm factors according to Martinec (1984),

$$N_{nm} = \sqrt{\frac{(2n+1)(n-m)!}{4\pi(n+m)!}} \tag{18}$$

and $P_n^m(\cos\vartheta)$ are the associated Legendre functions. Such a decomposition can be applied directly to the incremental gravitational potential $\varphi(\boldsymbol{r})$. Similarly, we can decompose the displacement vector to express also the remaining unknowns,

$$\boldsymbol{u}(\boldsymbol{r}) = u_r(\boldsymbol{r})\boldsymbol{e}_r + u_\vartheta(\boldsymbol{r})\boldsymbol{e}_\vartheta + u_\phi(\boldsymbol{r})\boldsymbol{e}_\phi, \tag{19}$$

$$u_r(\boldsymbol{r}) = \sum_{nm} U_{nm}(r) Y_{nm}(\vartheta, \phi), \tag{20}$$

$$u_\vartheta(\boldsymbol{r}) = \sum_{nm} V_{nm}(r) \frac{\partial Y_{nm}}{\partial \vartheta}(\vartheta, \phi) - W_{nm}(r) \frac{1}{\sin\vartheta} \frac{\partial Y_{nm}}{\partial \phi}(\vartheta, \phi), \tag{21}$$

$$u_\phi(\boldsymbol{r}) = \sum_{nm} V_{nm}(r) \frac{1}{\sin\vartheta} \frac{\partial Y_{nm}}{\partial \phi}(\vartheta, \phi) + W_{nm}(r) \frac{\partial Y_{nm}}{\partial \vartheta}(\vartheta, \phi), \tag{22}$$

$$\varphi(\boldsymbol{r}) = \sum_{nm} F_{nm}(r) Y_{nm}(\vartheta, \phi). \tag{23}$$

This formalism is in accord with Hanyk (1999) and Hanyk et al. (2002), where the problem of postglacial rebound is studied. If the vector spherical harmonic functions

$$\boldsymbol{S}_{nm}^{(-1)}(\vartheta, \phi) = Y_{nm} \boldsymbol{e}_r, \tag{24}$$

$$\boldsymbol{S}_{nm}^{(1)}(\vartheta, \phi) = \frac{\partial Y_{nm}}{\partial \vartheta} \boldsymbol{e}_\vartheta + \frac{1}{\sin\vartheta} \frac{\partial Y_{nm}}{\partial \phi} \boldsymbol{e}_\phi, \tag{25}$$

$$\boldsymbol{S}_{nm}^{(0)}(\vartheta, \phi) = -\frac{1}{\sin\vartheta} \frac{\partial Y_{nm}}{\partial \phi} \boldsymbol{e}_\vartheta + \frac{\partial Y_{nm}}{\partial \vartheta} \boldsymbol{e}_\phi, \tag{26}$$

are introduced, the displacement vector can be rewritten into the form

$$\boldsymbol{u}(\boldsymbol{r})=\sum_{nm}\left[U_{nm}(r)\boldsymbol{S}_{nm}^{(-1)}+V_{nm}(r)\boldsymbol{S}_{nm}^{(1)}+W_{nm}(r)\boldsymbol{S}_{nm}^{(0)}\right]. \tag{27}$$

$\boldsymbol{S}_{nm}^{(0)}$ create the toroidal basis and $\boldsymbol{S}_{nm}^{(-1)}$ a $\boldsymbol{S}_{nm}^{(1)}$ form the spheroidal basis. Let us denote the derivative in the direction of the radial coordinate by $f' \equiv \mathrm{d}f/\mathrm{d}r$. After the substitution of (5), (23) and (27) into the momentum equation (3) we obtain

$$\begin{aligned}\nabla\cdot\boldsymbol{\tau} &= \sum_{nm}\Bigg[\left(T'_{rr,nm}-\frac{4\gamma}{r^2}U_{nm}+\frac{2N\gamma}{r^2}V_{nm}+\frac{4\mu}{r\beta}T_{rr,nm}-\frac{N}{r}T_{r\vartheta,nm}\right)S_{nm}^{(-1)}\\ &\quad+\left(T'_{r\vartheta,nm}+\frac{2\gamma}{r^2}U_{nm}-\frac{N\gamma+(N-2)\mu}{r^2}V_{nm}+\frac{\lambda}{r\beta}T_{rr,nm}+\frac{3}{r}T_{r\vartheta,nm}\right)S_{nm}^{(1)}\\ &\quad+\left(T'_{r\phi,nm}-\frac{(N-2)\mu}{r^2}W_{nm}+\frac{3}{r}T_{r\phi,nm}\right)S_{nm}^{(0)}\Bigg], \end{aligned}\tag{28}$$

$$\begin{aligned}\boldsymbol{f} &= \sum_{nm}\Bigg[\left(\frac{4\rho_0 g_0}{r}U_{nm}-\frac{N\rho_0 g_0}{r}V_{nm}+\frac{(n+1)\rho_0}{r}F_{nm}-\rho_0 Q_{nm}\right)S_{nm}^{(-1)}\\ &\quad-\left(\frac{\rho_0 g_0}{r}U_{nm}+\frac{\rho_0}{r}F_{nm}\right)S_{nm}^{(1)}\Bigg], \end{aligned}\tag{29}$$

where $\boldsymbol{f}=-\rho_0\nabla\varphi+\nabla\cdot(\rho_0\boldsymbol{u})\nabla\varphi_0-\nabla(\rho_0\nabla\varphi_0\cdot\boldsymbol{u})$, $\beta=\lambda+2\mu$, $\gamma=\mu(3\lambda+2\mu)/\beta$, $N=n(n+1)$, $\nabla\varphi_0=g_0\boldsymbol{e}_r$ (with $g_0>0$) and

$$T_{rr,nm} = \beta U'_{nm}+\frac{\lambda}{r}\left(2U_{nm}-NV_{nm}\right), \tag{30}$$

$$T_{r\vartheta,nm} = \mu\left(V'_{nm}+\frac{U_{nm}-V_{nm}}{r}\right), \tag{31}$$

$$T_{r\phi,nm} = \mu\left(W'_{nm}-\frac{W_{nm}}{r}\right), \tag{32}$$

$$Q_{nm} = F'_{nm}+\frac{n+1}{r}F_{nm}+4\pi G\rho_0 U_{nm}. \tag{33}$$

$T_{rr,nm}$, $T_{r\vartheta,nm}$ a $T_{r\phi,nm}$ are the components of the traction,

$$\boldsymbol{e}_r\cdot\boldsymbol{\tau}=\sum_{nm}\left[T_{rr,nm}(r)\boldsymbol{S}_{nm}^{(-1)}+T_{r\vartheta,nm}(r)\boldsymbol{S}_{nm}^{(1)}+T_{r\phi,nm}(r)\boldsymbol{S}_{nm}^{(0)}\right]. \tag{34}$$

By substituting (23) and (27) into the Poisson equation (4) we obtain

$$\begin{aligned}\nabla\cdot(\nabla\varphi+4\pi G\rho_0\boldsymbol{u}) &= \sum_{nm}\Bigg[Q'_{nm}+4\pi G\frac{(n+1)\rho_0}{r}U_{nm}\\ &\quad-4\pi G\frac{N\rho_0}{r}V_{nm}-\frac{n-1}{r}Q_{nm}\Bigg]Y_{nm}. \end{aligned}\tag{35}$$

We do not neglect the inertial force in the momentum equation (3) and transform it into the Fourier spectral domain. In other words, we formally replace $\frac{\partial}{\partial t}$ by $i\omega$, where ω is the angular frequency of a tidal wave, to obtain $-\rho_0\omega^2\boldsymbol{u}$ on the right-hand side of (3). The index m will be omitted in the following text since it does not appear in the studied sets of equations.

4. Ordinary differential equations

In Section 3 the equations have been separated into two independent problems. The tidal displacement vector is described only by the spheroidal part, which satisfies the equation

$$(\nabla \times \boldsymbol{u}) \cdot \boldsymbol{e}_r = 0. \tag{36}$$

The unknown W_n representing the toroidal part is thus identically equal to zero in (21), (22), (27), (28) and (32) and the tidal displacement is described by only two unknowns U_n and V_n. Taking into account the expressions (28), (29) and (35), the momentum and the Poisson equations yield the system of three 2nd-order ODEs for the unknowns U_n, V_n and F_n,

$$\beta U_n'' + \frac{2\beta}{r}U_n' + \left(\frac{4\rho_0 g_0}{r} - 4\pi G\rho^2 - \frac{2\beta + \mu N}{r^2}\right)U_n - \frac{N}{r}(\lambda+\mu)V_n' + \tag{37}$$

$$+\left(\frac{3\mu+\lambda}{r^2} - \frac{\rho_0 g_0}{r}\right)NV_n - \rho_0 F_n' + \beta' U_n' + \frac{2\lambda'}{r}U_n - \frac{N\lambda'}{r}V_n \quad = \quad -\rho_0\omega_n^2 U_n,$$

$$\mu V_n'' + \frac{2\mu}{r}V_n' - \frac{\beta N}{r^2}V_n + \frac{\mu+\lambda}{r}U_n' + \left(\frac{2\beta}{r^2} - \frac{\rho_0 g_0}{r}\right)U_n - \tag{38}$$

$$-\frac{\rho_0}{r}F_n + \mu'\left(V_n' + \frac{1}{r}U_n - \frac{1}{r}V_n\right) \quad = \quad -\rho_0\omega_n^2 V_n,$$

$$F_n'' + \frac{2}{r}F_n' - \frac{N}{r^2}F_n + 4\pi G\rho_0\left(U_n' + \frac{2}{r}U_n - \frac{N}{r}V_n\right) + 4\pi G\rho_0' U_n \quad = \quad 0. \tag{39}$$

The boundary conditions (6)–(15), expressed for the unknowns U_n, V_n and F_n by means of (27) and (30)–(32), attain the form

$$\begin{aligned}
\text{solid-solid} \qquad & [U_n]_-^+ = 0, \\
& [V_n]_-^+ = 0, \\
& [T_{rr,n}]_-^+ \equiv \left[\beta U_n' + \frac{\lambda}{r}(2U_n - NV_n)\right]_-^+ = 0, \\
& [T_{r\vartheta,n}]_-^+ = \left[\mu\left(V_n' - \frac{V_n}{r} + \frac{U_n}{r}\right)\right]_-^+ = 0, \\
& [F_n]_-^+ = 0, \\
& [F_n' + 4\pi G\rho_0 U_n]_-^+ = 0,
\end{aligned} \tag{40}$$

$$
\begin{aligned}
\text{solid-liquid}\qquad & [U_n]_-^+ = 0,\\
& [T_{rr,n}]_-^+ \equiv \left[\beta U_n' + \frac{\lambda}{r}\,(2U_n - NV_n)\right]_-^+ = 0,\\
& [T_{r\vartheta,n}]_-^+ \equiv \mu\left(V_n' - \frac{V_n}{r} + \frac{U_n}{r}\right) = 0,\\
& [F_n]_-^+ = 0,\\
& [F_n' + 4\pi G\rho_0 U_n]_-^+ = 0,
\end{aligned}
\tag{41}
$$

$$
\begin{aligned}
\text{free surface}\qquad & T_{rr,n} \equiv \beta U_n' + \frac{\lambda}{r}\,(2U_n - NV_n) = 0,\\
& T_{r\vartheta,n} \equiv \mu\left(\frac{\mathrm{d}V_n}{\mathrm{d}r} - \frac{V_n}{r} + \frac{U_n}{r}\right) = 0,\\
& [F_n]_-^+ = 0,\\
& Q_n \equiv F_n' + \frac{n+1}{r}F_n + 4\pi G\rho_0 U_n = \frac{2n+1}{a}F_n^t\,,
\end{aligned}
\tag{42}
$$

where a denotes the radius of the free surface and F_n^t are spherical harmonic coefficients of the tidal potential φ_t. The right-hand side of the last boundary condition of (42) represents a source term where the tidal forcing comes to play. Let us clarify this equation. The incremental gravitational potential φ can be expressed as a sum of the gravitational potential φ_d caused by the deformation and the tidal potential φ_t,

$$
\varphi = \varphi_d + \varphi_t = \sum_{n=0}^{\infty}(F_n^d + F_n^t)Y_n\,. \tag{43}
$$

The boundary condition (15) relates the internal and external incremental gravitational potential at $r = a$ as follows,

$$
\left.\frac{\partial\varphi}{\partial r} + 4\pi G\rho_0 u\right|_{r=a_-} \;=\; \left.\frac{\partial\varphi}{\partial r}\right|_{r=a_+}\,. \tag{44}
$$

Outside the body, the coefficients F_n^d are proportional to $1/r^{n+1}$ (Jekeli 1989) and F_n^t are proportional to r^n (Agnew 2007). The right-hand side of (44) can thus be decomposed as follows,

$$
F_n^{d\prime} + F_n^{t\prime} = -\frac{n+1}{r}F_n^d + \frac{n}{r}F_n^t = -\frac{n+1}{r}F_n + \frac{2n+1}{r}F_n^t\,, \tag{45}
$$

that together with the left-hand side written simply as $F_n' + 4\pi G\rho_0 U_n$ forms the last condition of (42).

As usual (e.g., Wahr 1989), the n^{th}-degree contribution to $\boldsymbol{u}$ and φ on the surface can be related to the n^{th}-degree contribution $\varphi_{t,n} = F_n^t Y_n$ of the tidal potential φ^t by the definitions

$$u_{r,n}(\vartheta,\phi) = -\frac{h_n}{g_0}\varphi_{t,n}(\vartheta,\phi), \tag{46}$$

$$u_{\vartheta,n}(\vartheta,\phi) = -\frac{l_n}{g_0}\frac{\partial\varphi_{t,n}(\vartheta,\phi)}{\partial\vartheta}, \tag{47}$$

$$u_{\phi,n}(\vartheta,\phi) = -\frac{l_n}{g_0\sin\vartheta}\frac{\partial\varphi_{t,n}(\vartheta,\phi)}{\partial\phi}, \tag{48}$$

$$\varphi_n = \varphi_{d,n}(\vartheta,\phi) + \varphi_{t,n}(\vartheta,\phi) = (k_n+1)\varphi_{t,n}(\vartheta,\phi). \tag{49}$$

The dimensionless numbers h_n, l_n and k_n are called the tidal Love numbers. Carrying out the spherical decomposition of (46)–(49), we obtain the simple expressions

$$h_n = \frac{U_n}{a}\left(-\frac{ag_0}{F_n^t}\right), \tag{50}$$

$$l_n = \frac{V_n}{a}\left(-\frac{ag_0}{F_n^t}\right), \tag{51}$$

$$1+k_n = -\frac{F_n}{ag_0}\left(-\frac{ag_0}{F_n^t}\right). \tag{52}$$

The dimensionless factor $-ag_0/F_n^t$ can be used as a normalization constant for U_n, V_n and F_n. The last boundary condition of (42), multiplied by this factor, can be rewritten for the normalized unknowns into the final form,

$$\bar{F}_n' + \frac{n+1}{r}\bar{F}_n + 4\pi G\rho_0\bar{U}_n = -(2n+1)g_0, \tag{53}$$

that we use in numerical calculations. We employ the normalized unknowns $\bar{U}_n = -U_n a g_0/F_n^t$ etc. but we omit the bar for simplicity in the rest of the text. Relations (50)–(52) and boundary condition (53) are in accord with Fang (1998), where this normalization was implicitly made.

5. Matrix representation

Now we will discretize the studied BVP for the unknowns U_n, V_n and F_n to obtain a system of linear algebraic equations. The unknowns can be arranged into the vector

$$\boldsymbol{y} = (U_n, V_n, F_n)^{\mathrm{T}} \tag{54}$$

and the equations (37)–(39) can be rewritten into a matrix form,

$$\mathbf{A}(r)\cdot\boldsymbol{y}'' + \mathbf{B}(r)\cdot\boldsymbol{y}' + \mathbf{C}(r)\cdot\boldsymbol{y} = -\omega^2\mathbf{D}(r)\cdot\boldsymbol{y}, \tag{55}$$

where

$$\mathbf{A} = \begin{pmatrix} \beta & 0 & 0 \\ 0 & \mu & 0 \\ 0 & 0 & 1 \end{pmatrix}, \tag{56}$$

$$\mathbf{B} = \begin{pmatrix} \frac{2\beta}{r} + \beta' & -\frac{N(\lambda+\mu)}{r} & -\rho_0 \\ \frac{\mu+\lambda}{r} & \frac{2\mu}{r} + \mu' & 0 \\ 4\pi G\rho_0 & 0 & \frac{2}{r} \end{pmatrix}, \tag{57}$$

$$\mathbf{C} = \begin{pmatrix} \frac{4\rho_0 g_0}{r} - 4\pi G\rho_0^2 - \frac{2\beta+N\mu}{r^2} + \frac{2\lambda'}{r} & \frac{(\lambda+3\mu)}{r^2} - \frac{\rho_0 g_0}{r} & 0 \\ \frac{2\beta}{r^2} - \frac{\rho_0 g_0}{r} + \frac{\mu'}{r} & -\frac{N\beta}{r^2} - \frac{\mu'}{r} & -\frac{\rho_0}{r} \\ 4\pi G\left(\frac{2\rho_0}{r} + \rho_0'\right) & -\frac{4N}{r}\pi G\rho_0 & -\frac{N}{r^2} \end{pmatrix}, \tag{58}$$

$$\mathbf{D} = \begin{pmatrix} \rho_0 & 0 & 0 \\ 0 & \rho_0 & 0 \\ 0 & 0 & 0 \end{pmatrix}. \tag{59}$$

In order to discretize the equation (55) with a pseudospectral accuracy, we will follow the finite-difference approach designed by Fornberg (1996). The discretization grid comes out from the extrema of the Chebyshev polynomials $T_{M-1}(x)$ on the interval $\langle -1, 1\rangle$,

$$x_i = \cos\left(\frac{\pi(i-1)}{M-1}\right), \quad i = 1, .., M. \tag{60}$$

For a layer $r_{min} \leq r \leq r_{max}$ the Chebyshev grid consists of the points

$$r_i = r_{min} + \frac{r_{max} - r_{min}}{2}\left[\cos\left(\frac{\pi(i-1)}{M-1}\right) + 1\right], \quad i = 1, .., M. \tag{61}$$

The value of $\boldsymbol{y}$ and its derivatives at r_i are then expressed using the weighted sum of values $\boldsymbol{y}$ on the whole grid,

$$\boldsymbol{y}(r_i) = \sum_{j=1}^{M} \alpha_{ij}\boldsymbol{y}_j, \tag{62}$$

$$\boldsymbol{y}'(r_i) = \sum_{j=1}^{M} \beta_{ij}\boldsymbol{y}_j, \tag{63}$$

$$\boldsymbol{y}''(r_i) = \sum_{j=1}^{M} \gamma_{ij}\boldsymbol{y}_j, \tag{64}$$

where $\boldsymbol{y}_j = (U_n, V_n, F_n)^{\mathrm{T}}(r_j)$. The weight matrices α_{ij}, β_{ij} and γ_{ij} can be evaluated by means of the algorithm developed by Fornberg (1996). In this case $\alpha_{ii} = 1$, else $\alpha_{ij} = 0$. By employing (62)–(64) the equation (55) can be expressed in the form,

$$\sum_{j=1}^{M} [\mathbf{A}\gamma_{ij} + \mathbf{B}\beta_{ij} + \mathbf{C}\alpha_{ij}] \cdot \boldsymbol{y}_j = -\omega^2 \sum_{j=1}^{M} \mathbf{D}\alpha_{ij} \cdot \boldsymbol{y}_j. \tag{65}$$

It is necessary to explain how we understand the $\mathbf{A}\gamma_{ij}$ product in (65). The order of the matrix $\mathbf{A}$ is 3x3, whereas γ_{ij} is a matrix of order MxM. By multiplying each element of the matrix $\mathbf{A}$ with γ_{ij} we thus obtain the final $3M$x$3M$ matrix.

The interval $\langle r_{min}, r_{max}\rangle$ is divided into M points $r_{min} = r_1 < \ldots < r_M = r_{max}$ and three equations are needed at each of them. The equation (55) is used only at the internal points ($i = 2, .., M-1$) and the boundary conditions have to be satisfied at the two boundary points ($i = 1, M$). Thus, $3M - 6$ scalar equations (65) are for the internal points and the 3 equations have to be added at each boundary point as follows.

Let us first concern ourselves with the free surface, where the equations (42) normalized according to (53) are applied as

$$(T_{rr,n}, T_{r\vartheta,n}, Q_n)^{\mathrm{T}} = \mathbf{A}\cdot\boldsymbol{y}' + \mathbf{E}\cdot\boldsymbol{y} = \boldsymbol{q}. \tag{66}$$

The coefficient matrix $\mathbf{A}$ is given by (56), the matrix $\mathbf{E}$ has the form

$$\mathbf{E} = \begin{pmatrix} \frac{2\lambda}{r} & -\frac{N\lambda}{r} & 0 \\ \frac{\mu}{r} & -\frac{\mu}{r} & 0 \\ 4\pi G\rho_0 & 0 & \frac{n+1}{r} \end{pmatrix} \tag{67}$$

and the vector $\boldsymbol{q}$ is

$$\boldsymbol{q} = (0, 0, -(2n+1)g_0)^{\mathrm{T}}. \tag{68}$$

By substituting the relations (62)–(63) into (66), we obtain the 3 equations for the point r_{max}, which are in accord with the system of equations (65),

$$\sum_{j=1}^{M} [\mathbf{A}\beta_{Mj} + \mathbf{E}\alpha_{Mj}]\cdot\boldsymbol{y}_j = \boldsymbol{q}. \tag{69}$$

The boundary conditions are simple at the point of origin, i.e., at $r_{min} = 0$, where the equations $\boldsymbol{u}(r_{min}) = \mathbf{0}$ and $\varphi(r_{min}) = 0$ are satisfied. This condition can be expressed in the form,

$$\mathbf{I}\cdot\boldsymbol{y}_1 = \mathbf{0}, \tag{70}$$

where $\mathbf{I}$ is the identity matrix of order 3x3 and $\boldsymbol{y}_1 = (U_{n1}, V_{n1}, F_{n1})^{\mathrm{T}}$. Using the 3x3$M$ matrix $\mathbf{F}$,

$$\mathbf{F} = \begin{pmatrix} 1 & 0 & \ldots & \ldots & \ldots & \ldots & \ldots & \ldots & \ldots & \ldots \\ 0 & \ldots & \ldots & 1 & 0 & \ldots & \ldots & \ldots & \ldots & \ldots \\ 0 & \ldots & \ldots & \ldots & \ldots & \ldots & 1 & 0 & \ldots & \ldots \end{pmatrix}, \tag{71}$$

(70) can be rewritten into the form that corresponds to the set of equations (65) and (69),

$$\sum_{j=1}^{M} \mathbf{F}\cdot\boldsymbol{y}_j = \mathbf{0}. \tag{72}$$

If we consider a one-layer model, the whole problem is described by the system of equations (72), (65) and (69), which can be rewritten into the form,

$$\mathbf{P}\cdot\boldsymbol{y} = -\omega^2\mathbf{R}\cdot\boldsymbol{y} + \boldsymbol{q}, \tag{73}$$

where the vector $\boldsymbol{y} = (U_{n1}, \ldots, U_{nM}, V_{n1}, \ldots, V_{nM}, F_{n1}, \ldots, F_{nM})^{\mathrm{T}}$ has the order $3M$ and the matrices $\mathbf{P}$ and $\mathbf{R}$ are $3M$x$3M$,

$$\mathbf{P} = \begin{pmatrix} \mathbf{F} \\ \\ \mathbf{A}\gamma_{ij} + \mathbf{B}\beta_{ij} + \mathbf{C}\alpha_{ij} \\ \\ \mathbf{A}\beta_{Mj} + \mathbf{E}\alpha_{Mj} \end{pmatrix}, \quad \mathbf{R} = \begin{pmatrix} 0 \\ \\ \mathbf{D}\alpha_{ij} \\ \\ 0 \end{pmatrix}, \tag{74}$$

where $i = 2, .., M-1$ and $j = 1, .., M$.

The extension to more layers is quite simple. We start with the models composed of the solid layers only, the liquid layers will be discussed later. The vector $\boldsymbol{y}$ is marked $\boldsymbol{y}^{(k)}$ in the k^{th} layer. On the solid inner boundary between two layers the continuity conditions for the displacement, the gravitational potential, the traction and Q_n are described by (40). Using the expansions (62) and (63) we attain at the system

$$\sum_{j=1}^{M} \mathbf{I}\alpha_{Mj}^{(k)} \boldsymbol{y}_j^{(k)} - \sum_{j=1}^{M} \mathbf{I}\alpha_{1j}^{(k+1)} \boldsymbol{y}_j^{(k+1)} = \mathbf{0} \tag{75}$$

and

$$\sum_{j=1}^{M} \left[\mathbf{A}\beta_{Mj}^{(k)} + \hat{\mathbf{E}}\alpha_{Mj}^{(k)}\right] \boldsymbol{y}_j^{(k)} - \sum_{j=1}^{M} \left[\mathbf{A}\beta_{1j}^{(k+1)} + \hat{\mathbf{E}}\alpha_{1j}^{(k+1)}\right] \boldsymbol{y}_j^{(k+1)} = \mathbf{0}, \tag{76}$$

where the weight matrices are assigned to each layer. For brevity the coefficient matrices are written without the indexes, although they are layer-dependent. The index k will be omitted at the weight matrices as well. The matrix $\hat{\mathbf{E}}$ is

$$\hat{\mathbf{E}} = \begin{pmatrix} \frac{2\lambda}{r} & -\frac{N\lambda}{r} & 0 \\ \frac{\mu}{r} & -\frac{\mu}{r} & 0 \\ 4\pi G\rho_0 & 0 & 0 \end{pmatrix}. \tag{77}$$

The vector $\boldsymbol{Y}$ composed from the unknowns $\boldsymbol{y}_j^{(k)}$ from all layers can be defined as

$$\boldsymbol{Y} = \left(\boldsymbol{y}_1^{(1)}, \ldots, \boldsymbol{y}_M^{(1)}, \ldots, \boldsymbol{y}_1^{(k)}, \ldots, \boldsymbol{y}_M^{(k)}, \ldots, \boldsymbol{y}_1^{(K)}, \ldots, \boldsymbol{y}_M^{(K)}\right)^{\mathrm{T}}, \tag{78}$$

where K is the number of layers. Finally, the system of equations attains the form,

$$\mathbf{P} \cdot \boldsymbol{Y} = -\omega^2 \mathbf{R} \cdot \boldsymbol{Y} + \boldsymbol{Q}. \tag{79}$$

The matrices $\mathbf{P}$ and $\mathbf{R}$ have the order $3MK$x$3MK$ and the vector $\boldsymbol{Q}$ has $3MK$ components, where the last one contains the non-zero condition on the free surface,

$$\boldsymbol{Q} = [0, \ldots, 0, -(2n+1)g_0]^{\mathrm{T}}. \tag{80}$$

If the equations (72), (65), (75), (76) and (69) are arranged into the proper sequence, the $3MK$x$3MK$ matrix $\mathbf{P}$ for K layers has the form,

$$\mathbf{P} = \left(\begin{array}{llll}
\boxed{\mathbf{F}}_{3\text{x}3M} & & & \\
\boxed{\mathbf{A}\gamma_{ij} + \mathbf{B}\beta_{ij} + \mathbf{C}\alpha_{ij}}_{(3M-6)\text{x}3M} & & & \\
\boxed{\mathbf{A}\beta_{Mj} + \mathbf{E}\alpha_{Mj}}_{3\text{x}3M} & \boxed{-\mathbf{A}\beta_{1j} - \mathbf{E}\alpha_{1j}}_{3\text{x}3M} & & \\
 & & \ddots & \\
\boxed{\mathbf{I}\alpha_{Mj}}_{3\text{x}3M} & \boxed{-\mathbf{I}\alpha_{1j}}_{3\text{x}3M} & & \boxed{-\mathbf{A}\beta_{1j} - \mathbf{E}\alpha_{1j}}_{3\text{x}3M} \\
 & & \ddots & \\
 & & & \boxed{-\mathbf{I}\alpha_{1j}}_{3\text{x}3M} \\
 & & \ddots & \\
 & & & \boxed{\mathbf{A}\gamma_{ij} + \mathbf{B}\beta_{ij} + \mathbf{C}\alpha_{ij}}_{(3M-6)\text{x}3M} \\
 & & & \boxed{\mathbf{A}\beta_{Mj} + \mathbf{E}\alpha_{Mj}}_{3\text{x}3M}
\end{array} \right).$$

The matrix $\mathbf{R}$ is constructed by means of the matrix $\mathbf{D}$,

$$\mathbf{R} = \left(\begin{array}{llll}
\boxed{\mathbf{0}}_{3\text{x}3M} & & & \\
\boxed{\mathbf{D}\alpha_{ij}}_{(3M-6)\text{x}3M} & & & \\
\boxed{\mathbf{0}}_{3\text{x}3M} & \boxed{\mathbf{0}}_{3\text{x}3M} & & \\
\boxed{\mathbf{0}}_{3\text{x}3M} & \boxed{\mathbf{0}}_{3\text{x}3M} & \ddots & \boxed{\mathbf{0}}_{3\text{x}3M} \\
 & & \ddots & \boxed{\mathbf{0}}_{3\text{x}3M} \\
 & & \ddots & \boxed{\mathbf{D}\alpha_{ij}}_{(3M-6)\text{x}3M} \\
 & & & \boxed{\mathbf{0}}_{3\text{x}3M}
\end{array} \right).$$

The tangential components of traction automatically vanish inside the liquid material, where $\mu = 0$. Therefore, if the model contains such a layer, one equation at the liquid boundary is lost. Moreover, the component of the displacement V_n can be arbitrary, even a discontinuity is allowed over the liquid boundary. However, we can use the equation (38) at the boundary at the liquid side, where the zero shear modulus is employed,

$$\frac{\lambda}{r} U_n' + \left(\frac{2\lambda}{r^2} - \frac{\rho_0 g_0}{r} \right) U_n - \frac{N\lambda}{r^2} V_n - \frac{\rho_0}{r} F_n = -\rho_0 \omega_n^2 V_n. \qquad (81)$$

Thus we get back the right number of equations at the liquid boundary points and we can find V_n from the liquid side. If a boundary is formed by two different liquids, the tangential component of the traction vanishes inside both layers and another condition is lost. In such a case, the equation (81) has to be prescribed at the other side, too. The equation is included into the matrix $\mathbf{P}$ at the appropriate position in the same way as the rest of the equations. The system of the $3MK$ equations (79) can be rearranged to the form,

$$\left(\mathbf{P} + \omega^2 \mathbf{R}\right) \cdot \boldsymbol{Y} = \boldsymbol{Q} \tag{82}$$

and the final result is, hence, the non-homogeneous set of linear algebraic equations.

6. Numerical tests – Earth

The accuracy and efficiency of the presented method have been tested for the Preliminary Reference Earth Model (PREM) by Dziewonski and Anderson (1981). The PREM is a spherically symmetric model of density and seismic velocities (yielding thus also the Lamé parameters) prescribed in the form of polynomials up to the 3$^{\text{rd}}$ order in each of the 13 layers. For the present purpose we have removed the top oceanic layer and extended the 12th layer up to the radius of 6371 km. The tidal period is equal to the lunar value of 27.3 days.

The tidal Love numbers of degree 2 for total numbers of grid points ranging from 120 to 1300 are shown in Table 1. We have chosen a number of grid points in each layer so that the maximal distance between adjacent points of the Chebyshev grids would be as stated in Table 1. However, the minimal number of grid points in a layer is 10. The Love numbers converge to 5-digit accuracy for approximately 500 grid points. The CPU times on the Intel E8400 (3.0 GHz) processor can be also found in Table 1. Agnew (2007) lists the following values of tidal Love numbers for the PREM: $h_2 = 0.6032$, $l_2 = 0.0839$ and $k_2 = 0.2980$.

The tidal Love numbers of the PREM model for several spherical degrees are summarized in Table 2. The values were computed for 664 grid points. Let us note that the tidal Love numbers of the Gutenberg-Bullen model (Farrell 1972) differ by only about one percent.

grid points	max. distance [km]	h_2	l_2	k_2	CPU time [s]
122	200	0.60365	0.08401	0.29808	$\ll 1$
146	100	0.60366	0.08401	0.29809	$\ll 1$
202	50	0.60371	0.08401	0.29814	$\ll 1$
364	20	0.60372	0.08401	0.29814	2
664	10	0.60373	0.08402	0.29815	9
1292	5	0.60373	0.08402	0.29815	68

Table 1: Convergence and CPU times of tidal Love numbers with various grid densities. The tidal period is fixed to 27.3 days.

n	2	3	4	5	6
h_n	0.60373	0.28827	0.17524	0.12916	0.10712
l_n	0.08402	0.01480	0.01023	0.00847	0.00679
k_n	0.29815	0.09210	0.04148	0.02438	0.01682

Table 2: The tidal Love numbers for the Earth's model PREM.

7. Mars and Venus

We apply two models of density and seismic velocities after Sohl and Spohn (1997) to obtain the Martian tidal Love numbers. The first model was optimized to cosmochemical data (model A) and the other to satisfy the moment of inertia (model B). Both models yield the same surface gravitational acceleration of 3.7 ms^{-2} as well as a similar global structure: the crust, the upper and lower mantle separated by the transition zone of olivine to γ-spinel, and a liquid core. The layer of perovskite and the solid core are absent because suitable p-T conditions are not accomplished in the Martian interior. We adopt main boundaries from Sohl and Spohn (1997) and consider the density and the seismic velocities constant in each layer. The densities and the seismic velocities are shown in Fig. 1. In Table 3 we summarize the tidal Love numbers for $n = 2, 3, 4$ computed for the tidal frequency of Phobos. The obtained results clearly demonstrate the sensitivity of tidal Love numbers to changes of the core radius.

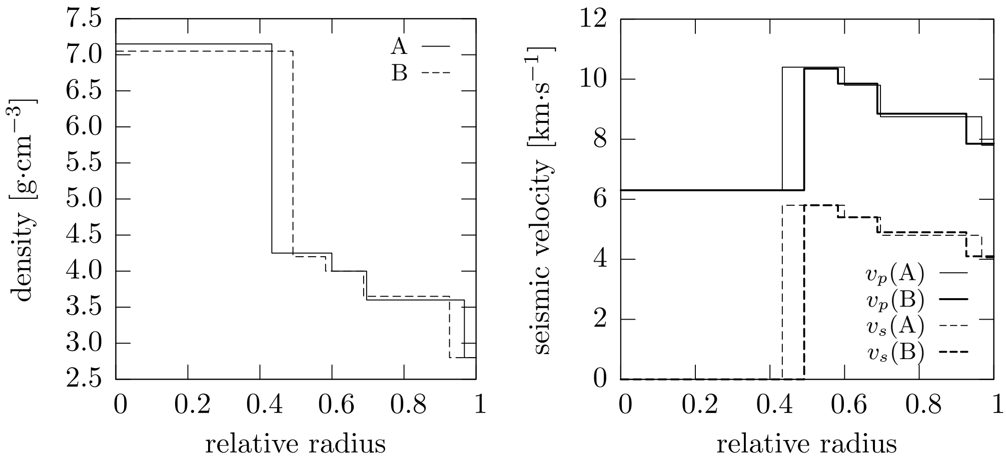

Figure 1: Parameters of the Martian models adopted from Sohl and Spohn (1997).

n	Model A h_n	Model A l_n	Model A k_n	Model B h_n	Model B l_n	Model B k_n
2	0.172	0.036	0.093	0.212	0.038	0.113
3	0.083	0.010	0.031	0.095	0.008	0.034
4	0.057	0.005	0.016	0.060	0.004	0.016

Table 3: The Love numbers for the two models of Mars.

Venus, with a radius of 6051 km, is only slightly smaller than the Earth, but the small difference in size may have important consequences for its interior. First, plate tectonics does not exist on Venus and the approximately 100-km thick lithosphere covers the surface of the planet as a lid. Konopliv and Sjogren (1994) estimated the average thickness of the Venus' crust to be about 35 km. Slow rotation of Venus does not satisfactorily explain the lack of its magnetic field (Phillips and Russell 1987). In the Venus' core the phase-transition conditions for crystallization of iron are probably not accomplished and thus chemical convection need not exist (Stevenson 1983) even if there is a liquid core. Zábranová (2008) preferred a model divided into the 5 layers: the crust, the upper and lower mantle separated by the transition zone and the liquid core, where the interfaces are adopted from Schubert et al. (2001) and values of densities and seismic velocities were constructed in an analogy to the Earth. This model satisfies the observed gravitational acceleration at the surface equal to 8.87 ms^{-2}. The model densities and the seismic velocities are shown in Fig. 2.

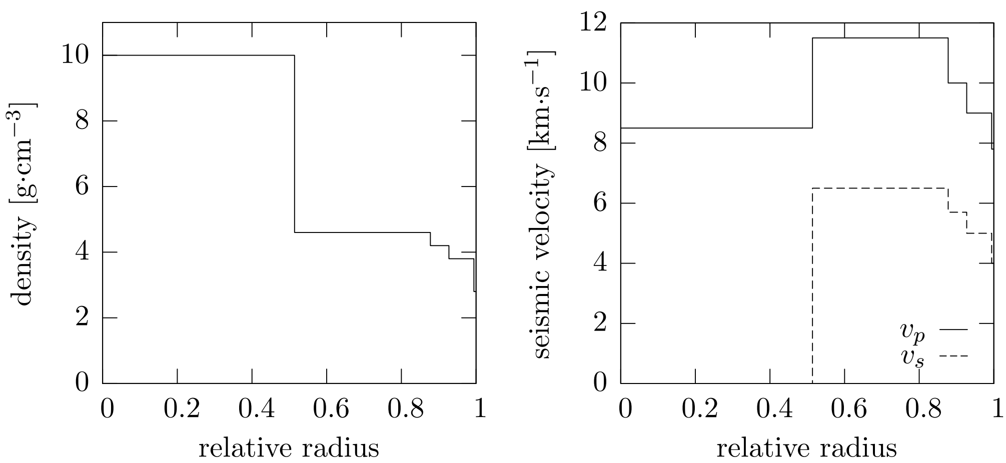

Figure 2: Parameters of the Venusian model (Zábranová, 2008).

In Table 4 we summarize the tidal Love numbers for $n = 2, 3, 4$. The Love number k_2 is determined from the time variations in the gravitational coefficients C_{22} and

S_{22} at the solar period. Konopliv and Yoder (1996) have found $k_2 = 0.295 \pm 0.066$, which is in good agreement with our value, and is thus an argument for the existence of the liquid core in Venus.

n	h_n	l_n	k_n
2	0.550	0.082	0.281
3	0.261	0.014	0.089
4	0.160	0.008	0.041

Table 4: The Love numbers for the model of Venus.

8. Concluding remarks

We have presented a new numerical method for evaluating the tidal Love numbers of prestressed elastic spherically symmetric bodies. While the traditional approach is based on the propagation of particular solutions of six 1^{st}-order differential equations in the radial direction by Runge-Kutta techniques, we have proposed direct discretization of the boundary value problem for three 2^{nd}-order differential equations (37)–(42) by high-accuracy finite-difference pseudospectral schemes that results in a system of linear algebraic equations (82). Chebyshev grids have been employed in each layer, where the model parameters are continuous, that makes the matrix of the algebraic system almost block diagonal (the ABD matrix). Special solvers (e.g., `f01lhf` from the NAG library) are designed for such matrices. An advantage of preserving 2^{nd}-order equations is that a half-size algebraic system is to be solved. On the other hand, derivatives of the model parameters are required, but this is trivial for models with piecewise constant parameters and easy for the polynomials of the PREM model.

We have discussed that care must be taken in assembling algebraic equations (83) for models with the liquid core. Nevertheless, the system becomes singular in the zero-frequency limit. Such a behavior is a numerical manifestation of a fundamental gravitational instability of compressible elastic liquids. This difficulty, also known as the Longman paradox (Longman 1963; Chinnery 1975), is enlightened in detail by Fang (1998) and we avoid it by keeping realistic non-zero tidal frequencies.

A generalized eigenvalue problem with matrices **P** and **R** can provide us with periods of free oscillations (Zábranová 2008) of studied models. Together with rapid evaluation of tidal Love numbers by the presented method, this combined matrix approach may serve as an efficient numerical tool in structural studies of planetary bodies.

Acknowledgements. E. Z. cordially acknowledges the remaining authors for sharing their reminiscences of Beethovenian impression from discussions of Prof. Milan Burša with members of the Department of Geophysics—especially with Prof. Karel Pěč—that helped substantially in the orientation of a part of the department research towards the Earth's gravity field and related studies on the internal dynamics and structure of the Earth. This contribution was motivated by the fact that the study of the tidal potential is one of the key research interests of Prof. Burša, e.g., Burša (1993), Burša and Pěč (1993), Burša and Kostelecký (1999). We thank Ondřej Souček for his skills in the field of the functional analysis and also Kateřina Topilová for her help with writing. This research has been supported by the research project MSM 0021620860 of the Czech Ministry of Education.

References

Agnew, D. C., 2007. Earth tides, in *Treatise on Geophysics, Vol. 3: Geodesy*, ed. by Herring T., Elsevier, Amsterdam etc., pp. 163–195.

Burša, M., 1993. Tidal potential due to general bodies, *Earth, Moon and Planets, Vol. 62*, 2, 139–144.

Burša, M. and Pěč, K., 1993. *Gravity Field and Dynamics of the Earth*, Springer–Verlag Berlin, Heidelberg.

Burša, M. and Kostelecký, J., 1999. *Space Geodesy and Space Geodynamics*, Ministry of Defence of the Czech Republic, Prague.

Chinnery, M. A., 1975. The static deformation of an Earth with a fluid core: A physical approach, *Geophys. J. R.*, 42, 461–475.

Dahlen, F. A. and Tromp, J., 1998. *Theoretical Global Seismology*, Princeton University Press, Princeton.

Dziewonski, A. M. and Anderson, D. L., 1981. Preliminary reference Earth model, *Phys. Earth Planet. Inter.*, 25, 297–356.

Fang, M., 1998. Static deformation of the outer core, in *Dynamics of the Ice Age Earth: A Modern Perspective*, ed. by P. Wu, Trans Tech Publ., Zürich, pp. 155–190.

Fornberg, B., 1996. *Practical Guide to Pseudospectral Methods*, Cambridge University Press, New York.

Hanyk, L., 1999. *Viscoelastic Response of the Earth: Initial-value Approach*, PhD Thesis, Faculty of Mathematics and Physics, Charles University in Prague. `http://geo.mff.cuni.cz/theses.htm`

Hanyk, L., Matyska, C. and Yuen, D. A., 2002. Determination of viscoelastic spectra by matrix eigenvalue analysis, in *Ice Sheets, Sea Level and the Dynamic Earth*, ed. by Mitrovica, J. X. and Vermeersen, B. L. A., Geodynamics Series, 29, AGU, Washington, pp. 257–273.

Jekeli, Ch., 1989. Earth's external gravity field, in *The Encyclopedia of Solid Earth Geophysics*, ed. by James, D. E., VNR, New York, pp. 322–331.

Kobayashi, N., 2007. A new method to calculate normal modes, *Geophys. J. Int.*, 168, 315–331.

Konopliv, A. S. and Sjogren, W. L., 1994. Venus spherical harmonic gravity model to degree and order 60, *Icarus*, 112, 42–54.

Konopliv, A. S. and Yoder, C. F., 1996. Venusian k_2 tidal Love number from Magellan and PVO tracking data, *Geophys. Res. Lett.*, 23, 1857–1860.

Longman, I. M., 1963. A Green's function for determining the deformation of the Earth under surface mass loads, 2. Computations and numerical results, *J. Geophys. Res.*, 68, 485–496.

Martinec, Z., 1984. Free oscillations of the Earth, *Travaux Géophys.*, 591, 117–236.

Martinec, Z., 1999. Spectral, initial value approach for viscoelastic relaxation of a spherical earth with a three-dimensional viscosity–I. Theory, *Geophys. J. Int.*, 137, 469–488.

Martinec, Z., 2000. Spectral-finite element approach to three-dimensional viscoelastic relaxation in a spherical earth, *Geophys. J. Int.*, 142, 117–141.

Melchior, P., 1978. *The Tides of the Planet Earth*, Pergamon Press, Oxford.

Phillips, J. L. and Russell, C. T., 1987. Upper limit on the instrinsic magnetic field of Venus, *J. Geophys. Res.*, 92, 2253–2263.

Schubert, G., Turcotte, D. L. and Olson, P., 2001. *Mantle Convection in the Earth and Planets*, Cambridge University Press, United Kingdom.

Sohl, F., and Spohn, T., 1997. The interior structure of Mars: Implications from SNC meteorites, *J. Geophys. Res.*, 102, 1613–1635.

Stevenson, D. J., Spohn, T. and Schubert, G., 1983. Magnetism and thermal evolution of the terrestrial planets, *Icarus*, 54, 466–489.

Wahr, J. M., 1989. Earth tides, in *The Encyclopedia of Solid Earth Geophysics*, ed. by James, D. E., VNR, New York, pp. 359–363.

Zábranová, E., 2008. *Free Oscillations and Tides of Moons and Planets*, MSc Thesis, Faculty of Mathematics and Physics, Charles University in Prague. `http://geo.mff.cuni.cz/theses.htm`